

Experimental investigation of band structure modification in silicon nanocrystals

B. J. Pawlak, T. Gregorkiewicz, and C. A. J. Ammerlaan

Van der Waals-Zeeman Institute, University of Amsterdam, Valckenierstraat 65, 1018 XE Amsterdam, The Netherlands

W. Takkenberg

Biology Department, University of Amsterdam, Kruislaan 316, 1098 SM Amsterdam, The Netherlands

F. D. Tichelaar

National Center for High Resolution Electron Microscopy, Rotterdamseweg 137, 2628 AL Delft, The Netherlands

P. F. A. Alkemade

DIMES, Delft University of Technology, Lorentzweg 1, 2600 GA Delft, The Netherlands

(Received 5 July 2000; revised manuscript received 15 March 2001; published 27 August 2001)

Experimental studies of size-related effects in silicon nanocrystals are reported. We present investigations carried out on nanocrystals prepared from single-crystal Si:P wafer by ball milling. The average final grain dimension varied depending on the way of preparation in the range between 70 and 230 nm. The ball milling was followed by sedimentation and selection of the smallest grains. The initial grain size distribution was measured by scanning electron microscopy. Further reduction in size was achieved by oxidation at 1000 °C which creates a silicon dioxide layer around a silicon core. The oxidation process was monitored by transmission electron microscopy and the growth speed of SiO₂ was estimated in order to model the grain size of nanocrystals. Crystallinity of silicon grains was confirmed by x-ray diffraction and by transmission electron microscopy using a bright/dark field method and selected area diffraction pattern. In the silicon nanocrystals the electron energy levels are shifted which was observed separately for conduction band, valence band and energy band gap. Electron paramagnetic resonance was applied to investigate variation of the conduction band minimum by monitoring its influence on the hyperfine interaction of phosphorus shallow donor. On the basis of these results an explicit expression for conduction band upshift as a function of average grain size has been derived. Information about the downshift of the valence band was obtained from measurements on a photoluminescence band related to a deep to shallow level transition. A perturbation of a few meV for grain sizes of the order about 100 nm has been observed. Internal consistency of these findings has been examined by investigation of the photoluminescence band due to an electron-hole recombination whose energy is directly related to the band gap of silicon.

DOI: 10.1103/PhysRevB.64.115308

PACS number(s): 73.23.-b, 73.22.-f, 76.30.-v, 78.55.-m

I. INTRODUCTION

Silicon is the main semiconductor used by the electronics industry. Presently intensive research on silicon is focused on modifications that would enable its light generation. The primary aim of both theoretical and experimental investigations of silicon nanocrystals is to elucidate the origin of visible light emission, which is often observed in grains with diameters of the order of a few nanometers. This paper reports on experiments in which the influence of grain size on the silicon band structure is observed. Investigations conducted on silicon nanocrystals have shown that decreasing size or lowering dimensionality of silicon produce a variety of interesting effects. In small crystallites¹ often quantum confinement effect is observed. This enlarges the bandgap energy,² and in case of silicon, can possibly also lead to change of its character from indirect to direct.³ Grains of the order of a few nanometers are considered to be crystalline and the effects related to the band structure perturbations in such powders were investigated by various optical techniques. In photoluminescence (PL) increased efficiency of excitonic emission and its gradual shift to higher energies upon size reduction have been experimentally observed.^{4,5} Light emission with

the energy exceeding the band gap of bulk silicon has been reported in nanocrystals of a few-nanometers size. Any experiment conducted on few-nanometer silicon grains is sensitive to surface effects in an unpredictable way. Surface-to-volume ratio in such crystals becomes considerable and unavoidably leads to entanglement of volume- and surface-related effects. Consequently, in experimental practice surface-related effects obscure observation and conclusive identification of effects related to the restricted volume of nanocrystals. The most studied nanocrystals are prepared by electroetching in the form of so-called porous silicon. Results of research conducted on porous silicon and aiming at explanation of the PL origin are often contradicting each other. Visible PL has been associated by Canham⁵ and Behrensmeier *et al.*⁶ with bulk properties of nanocrystals. Other studies, however, explain it by chemical bonds on the surface. Also a report of Brandt *et al.*⁷ identifies siloxene derivatives as the source of the visible room-temperature PL in porous silicon. Comprehensive comparisons of light emission from porous silicon and siloxene derivatives are found in articles of Fuchs *et al.*⁸ and Stutzmann *et al.*⁹ In view of such a controversy the main challenge for investigations of silicon nanocrystals is to elucidate the origin of the visible PL.

In the present study we investigate spatial confinement related phenomena in Si nanocrystals prepared by ball milling. Photoluminescence properties of silicon nanocrystals prepared by ball milling were previously studied by Shen *et al.*¹⁰ Here we present evidence of a smooth transition between bulk and nanocrystalline properties of silicon. By observation of defects characteristic for bulk crystal, we trace their behavior as slightly perturbed by volume restriction. The research is conducted by techniques in which the surface and surface-related defects do not play the dominant role; consequently the observed effects may be associated with bulk properties of the sample. We present experimental evidence of shifts of the electron energy bands in the relatively large crystallites for which the theoretically estimated spatial confinement induced changes—conduction band upshift and valence band downshift, both resulting in enlargement of the energy band gap—should be of the order of a few meV only. Si powders prepared in the current study by mechanical ball-milling were extensively characterized by various experimental techniques in order to check their quality and suitability for the undertaken research. Experimental techniques of electron paramagnetic resonance (EPR) and PL have been used. The investigations were aimed at observation of the spatial confinement effect for the band gap and, separately, for conduction and valence band edges.

(1) *Conduction band.* EPR was used to observe modification of the electronic structure of the phosphorus impurity. Substitutional phosphorus in silicon forms an effective-mass-theory (EMT) donor whose electronic structure is related to the conduction band minima. The extended character of the donor electron wave function renders this center sensitive to spatial confinement. The phosphorus donor in bulk silicon is paramagnetic in its neutral charge state P^0 and is well studied by EPR. It has cubic symmetry, which is advantageous for the presented case of mechanically milled silicon where the grains are randomly oriented. From the EPR spectrum details of the wave function—spin localization on the phosphorus nucleus and mutual overlap of neighboring donors—can be concluded. At the same time the investigated EPR spectrum is exclusive for a substitutional donor and therefore only the bulk of the nanocrystal is monitored. In that way the volume and the surface effects can be separated. This is a clear advantage when compared to other less discriminative techniques as used in the present and in earlier studies.^{11,12}

(2) *Valence band.* The effect of spatial confinement has been observed on a photoluminescence line at $E \approx 820$ meV corresponding to a deep to shallow level transition. Guided by the energy of the emission and by the sample preparation method the luminescence can be attributed to the dislocation-related optical center D1. The PL emission related to dislocation has been investigated before by Drozdov *et al.*,¹³ Sauer *et al.*,¹⁴ and Suezawa *et al.*¹⁵ Several lines were observed and interpreted as radiative transitions between a deep level and a shallow level related to the valence band. Under the assumption that the band variations have a more pronounced effect on the shallow rather than the deep level position, the increase in transition energy upon grain downsizing can be mainly assigned to downshift of the valence band.

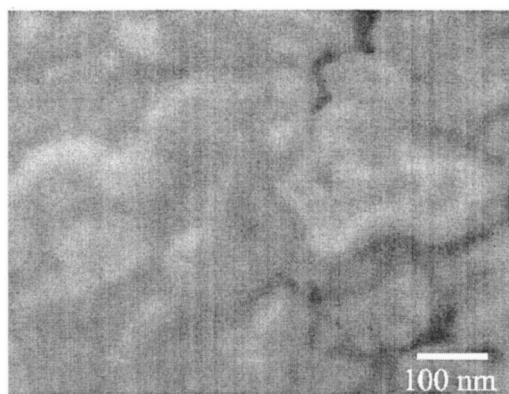
(3) *Band gap.* Variation of the silicon band gap has been directly measured from the energy of an electron-hole recombination. For the particular recombination observed in the experiment a full structure consisting of a no-phonon transition followed by TA and TO phonon replicas was observed. The experiment showed gradual blue shift of the recombination energy of this band by 16 meV for grain sizes between 115 and 75 nm. In our interpretation this change reflects increase of the band gap energy.

Perturbations deduced for each band and band gap were compared for internal consistency.

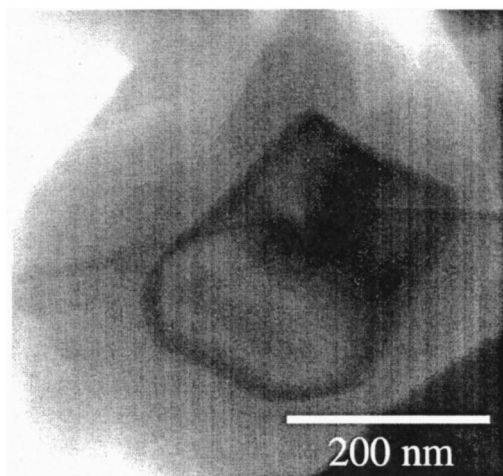
II. SAMPLES

Phosphorus-doped Czochralski (Cz) silicon with a doping level $[P] = 5 \times 10^{15} \text{ cm}^{-3}$ has been used for preparation of nanocrystals. A ball-milling production method has been explored, resulting in grains of perfect crystallinity and various sizes.

Mechanical ball milling followed by sedimentation stages is an efficient technique for preparation of silicon nanocrystals. It has been developed in our laboratory to produce grains of the order of 100 nanometers dimensions. Mechanical ball milling of silicon wafers has been performed in a ZrO_2 crucible with a set of balls from the same material. Typical milling time was 30 mins. ZrO_2 balls and Si powder were immersed in ethanol in order to prevent charging. The milling step was followed by free sedimentation for 20 h in order to remove the largest silicon grains. Only those which formed powder-ethanol suspension at room temperature were collected for further processing. The suspension was then transferred to an ultrasonic cleaner. Our experience showed that application of ultrasonic vibrations serves as an efficient tool to divide grain agglomerations into individual crystallites. This proved to be very crucial for further size segregation. Centrifuged sedimentation is a mass segregation method that does not distinguish between a single big grain and an aggregate of smaller particles. Therefore the centrifuging was preceded by ultrasonic vibrations for efficient size segregation. Scanning electron microscopy (SEM) images of various fractions of powders gave information about size distribution of grains—see Fig. 1(a). The distributions obtained by counting grains of different sizes (700 counts per photo), were fitted with the usual function $\exp[-\ln^2(d/z)/2w^2]$, in which d is the grain size and w is a parameter describing the width of the distribution. For the particular five sets of powders investigated in this study by EPR and PL the maxima of size distributions were determined at $z_1 = 200$ nm for big, $z_2 = 110$ nm for medium big, $z_3 = 100$ nm for medium small, $z_4 = 80$ nm for small and $z_5 = 60$ nm for very small nanocrystals. The width parameter was found to be around $w = 0.6$ for all the investigated powders. Further size reduction was achieved by oxidation of grains. The powders were annealed at 1000°C in open air for time durations from 5 min to 2 h. By such a procedure the silicon core of each grain is reduced by formation of a SiO_2 layer. At the same time silicon surface is replaced by Si/SiO_2 interface. Creation of Si/SiO_2 interface reduces the concentration of unsaturated bonds and is very advantageous



(a)



(b)

FIG. 1. (a) Scanning electron microscopy image of silicon ball-milled grains. (b) Transmission electron micrograph of part of a silicon grain oxidized at 1000 °C for 2 h. Crystalline silicon in the middle, dark part of the figure, amorphous SiO₂ layer surrounding the silicon core.

for further studies. In case of both techniques, EPR and PL, the dangling bonds give rise to additional signals obstructing information pertinent to the band structure changes.

Figure 1(b) presents a transmission electron microscopy (TEM) image of an oxidized silicon grain as used in the present study; both the crystalline Si core and the external layer of SiO₂ developed by oxidation can be readily seen. By TEM we could also monitor the growth speed of the SiO₂ layer. We conclude that the growth process proceeds according to the well established formula $d_{\text{SiO}_2} = 10.78\sqrt{t}$ (for oxidation at 1000 °C in air), where d_{SiO_2} is the oxide layer thickness (in nanometers) and t is the oxidation time (in minutes).¹⁶ Additional information about chemical composition was obtained from energy dispersive spectrum (EDS), from which the stoichiometry of the surrounding layer was found to match silicon dioxide (SiO₂). Further, the TEM-related techniques established the amorphous structure of the SiO₂.

The intention of this study was to observe perturbations of the silicon band structure. However, only small effects can

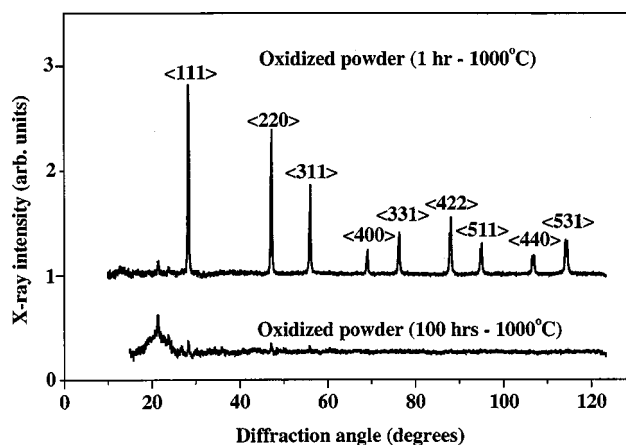


FIG. 2. X-ray diffraction patterns of oxidized silicon powders showing lines characteristic for crystalline silicon. Prolonged annealing reduces the intensity of diffracted lines. Hundred hours annealing converts all the silicon into silicon dioxide. The two x-ray patterns have been offset in order to distinguish them.

be expected for grain sizes of around 100 nm as prepared by mechanical milling. For the purpose of the study it is of crucial importance to ascertain that the changes originate from the size-related effect and are not influenced by other factors, such as silicon crystal structure transitions or amorphization. The crystallinity of silicon powders was examined by x-ray diffraction. The result is shown in Fig. 2. Characteristic diffraction patterns of crystalline silicon were clear and strong for as-milled as well as for oxidized nanocrystals. Their intensity gradually decreased upon heat-treatment indicating size reduction of the silicon core. After prolonged oxidation the x-ray pattern vanished completely as all the silicon was transformed into SiO₂. For the largest grains x-ray diffraction has also been applied successfully as a tool for grain size estimation. On the basis of diffraction lines broadening we could conclude that all the grains used in the study were smaller than 1 μm . The measured positions of the diffraction lines did not depend on the oxidation time, indicating that the growth of silicon dioxide did not affect the silicon lattice constant.

In addition to Röntgen diffraction, grain crystallinity was confirmed by TEM experiments, bright-field/dark-field (BF/DF) imaging and selected area diffraction pattern (SADP) analysis. We obtained clear evidence that both as-milled and oxidized silicon grains retain their diamond structure characteristic for the bulk material. The intensity distribution in BF/DF images showed that the cores of the powder particles were fully crystalline up to the Si/SiO₂ interface.

In our investigation the electronic structure behavior of phosphorus shallow donor was traced by EPR. As already mentioned, reduction of average grain size was achieved by oxidation. As known from the literature, oxidation of silicon may produce a modest pile-up of phosphorus at the Si/SiO₂ interface.¹⁷ In order to verify the influence of oxidation on phosphorus distribution, a dedicated investigation of impurity distribution by secondary ion mass spectroscopy (SIMS) has been performed. Special care has been taken to distinguish signals from ³¹P and ³⁰SiH. Figure 3 presents [P] pro-

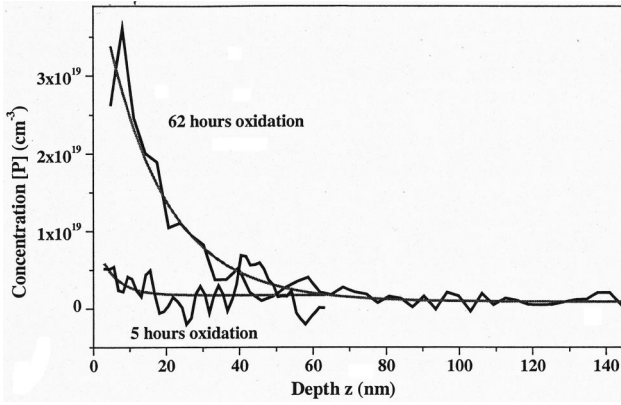


FIG. 3. Secondary ion mass spectroscopy of a heavily doped silicon wafer ($[P]=10^{18} \text{ cm}^{-3}$) oxidized for 5 and 62 h. The pile-up is clearly visible only for 62 h. oxidation. The fitting parameters are given in Table I.

files in two silicon wafers prepared especially for this experiment. In this case the phosphorus profiles were measured in Si material with a high phosphorus concentration ($[P] \approx 1 \times 10^{18} \text{ cm}^{-3}$) which was oxidized for much longer times (5 and 62 h) than used in the preparation of powders. Both $[P]$ profiles have been fitted with the standard function $[P(z)] = [P]_s \exp(-z/Z) + [P]_b$, where the parameters for the two oxidation times are gathered in Table I. It has been concluded that only the wafer oxidized for the longer time (62 h) showed significant pile-up at the interface. The powder material used in our EPR experiment had more than two orders of magnitude lower phosphorus concentration ($[P]=5 \times 10^{15} \text{ cm}^{-3}$) and its time of oxidation did not exceed 2 h. Therefore we conclude that the phosphorus pile-up effect is negligible for the investigated Si powder samples.

III. SPATIAL CONFINEMENT

The investigation of silicon nanocrystals was intended to cover shifts of conduction band, valence band, and band gap related to spatial confinement. In line with that goal, the experimental methods of EPR and PL with the observation of donor, acceptor centers and excitons were applied.

A. Electron paramagnetic resonance

Crystals obtained by ball milling retain their crystalline structure. Since the production of the nanocrystals is not related to clustering from single atoms but to size reduction of initially bulk material, the phosphorus position is not affected in the lattice. From the EPR spectrum we find evidence that phosphorus atoms are embedded inside of Si nanocrystals on the regular substitutional sites.

The behavior of the conduction band was investigated by its influence on the phosphorus hyperfine interaction. The measurements were performed at a temperature of $T = 4.2 \text{ K}$ in a superheterodyne EPR spectrometer operating at 23 GHz in the K -microwave band and tuned to detect the dispersive part of the signal. In that way the EPR technique has been applied to investigate size-related effects. The EPR of the P donor in bulk Si has been extensively investigated in

TABLE I. Parameters describing the phosphorus concentration $[P(z)]$ as a function of depth z after 5 and 62 h oxidation at 1000°C in air. The concentration profile has been fitted with the function $[P(z)] = [P]_s \exp(-z/Z) + [P]_b$.

Oxidation time (h)	$[P]_s (\text{cm}^{-3})$	$Z (\text{nm})$	$[P]_b (\text{cm}^{-3})$
5	$(8 \pm 3) \times 10^{18}$	5 ± 3	$(1.8 \pm 0.5) \times 10^{18}$
62	$(44 \pm 8) \times 10^{18}$	16 ± 3	$(0.9 \pm 0.2) \times 10^{18}$

experiment by Feher *et al.*¹⁸ and in theory by Kohn and Luttinger.¹⁹ The spectrum consists of two lines separated by $A/g\mu_B = 4.20 \text{ mT}$ due to the hyperfine interaction. In the experiment we measure the magnitude of the hyperfine constant A for different grain sizes. It is proportional to the localization of electron wave function on the phosphorus nucleus and is given by the Fermi contact term $A = \frac{2}{3} \mu_0 g \mu_B g_N \mu_N |\Psi(0)|^2$. In Fig. 4(a) we present EPR spectra of the bulk Cz-Si:P material and ball-milled nanocrystals.

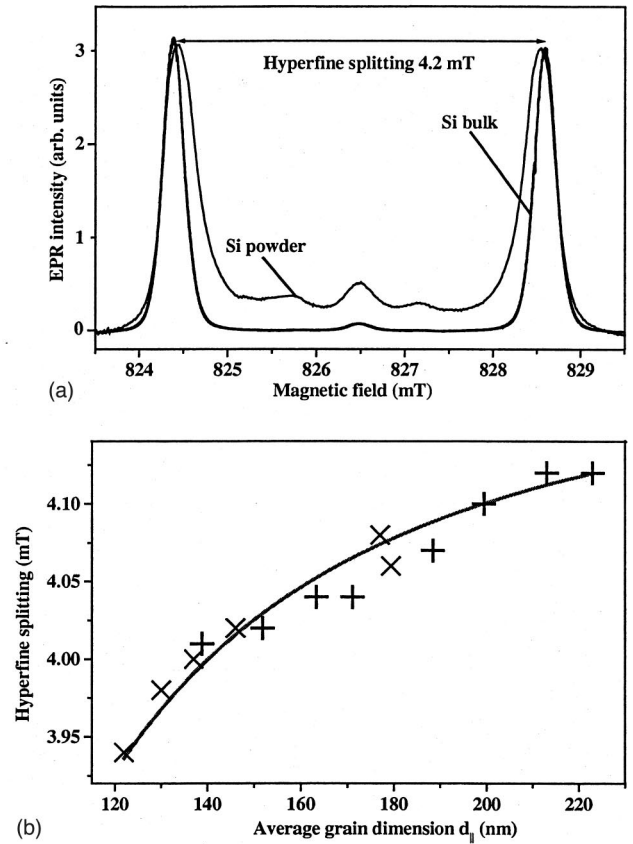


FIG. 4. (a) EPR spectrum of the Cz-Si:P ($[P]=5 \times 10^{15} \text{ cm}^{-3}$) bulk and oxidized ball-milled nanocrystal sample. Two hyperfine lines and small peaks originating from mutual overlap between individual donors appear for the milled sample. Spectra are taken at a microwave frequency $\nu = 23.11997 \text{ GHz}$. (b) Hyperfine splitting parameter for the two smallest series of powders, $z_4 = 80 \text{ nm}$ (indicated by “+”), $z_5 = 60 \text{ nm}$ (indicated by “x”) after different oxidation stages versus average grain diameter $d_{||}$. For bulk silicon $A/g\mu_B = 4.20 \text{ mT}$. For powders the hyperfine parameter decreases with diminishing average grain diameter. The solid line represents a fit to the experimental data.

For the early report on EPR investigations of Si powders, see Ref. 20. The hyperfine lines originating from phosphorus in nanocrystalline material are shifted with respect to the bulk spectrum and asymmetrically broadened toward each other, indicating a smaller hyperfine interaction A . In Fig. 4(b) results of systematic EPR measurements of oxidized samples are summarized. A gradual decrease of the hyperfine parameter A versus average silicon grain volume is concluded. The correlation between average grain volume and hyperfine splitting is independent on the SiO_2 thickness as observed in experiment when investigating nanocrystals of equal dimension, but with different initial grain size distribution and different oxidation times. It is known from the literature that the growth of SiO_2 on Si wafer produces stress in the vicinity of the Si/SiO₂ interface.²¹ The local stress at the Si/SiO₂ interface created during oxidation at 1000 °C can be of the order of $\sigma = 10^6$ dynes/cm², which is less than the uniaxial stress applied by Wilson and Feher²² for the perturbation of silicon band structure. In the case of the oxidized silicon grains the oxide is surrounding the silicon symmetrically so no preferable direction is distinguished. As described by Charitat and Martinez²¹ the stress diminishes with increasing distance from the SiO₂/Si interface, thus it cannot be responsible for the effect present in the bulk of the nanocrystal. Additionally, the oxidation-induced stress is efficiently relaxed by point defect generation. Therefore a possible explanation in terms of stress induced by the external oxide layer is not raised.

The relation between the hyperfine splitting parameter A and average grain volume is analyzed in terms of spatial confinement. In the present analysis the reduction of A is an effect of limited size of Si grain and its asymmetrical shape. The behavior of phosphorus donor in silicon is well understood within the EMT.¹⁹ The phosphorus donor electron wave function is described as a linear combination with coefficients $\alpha^{(j)}$ of products of an envelope function $F^{(j)}(r)$ —the solution of a hydrogenlike Schrödinger equation—and a Bloch function $\psi^{(j)}(r) = u^{(j)}(r)\exp(ik_0^{(j)}r)$, where j enumerates the valleys in the sixfold degenerate conduction band minimum of silicon. The probability of finding an electron in the j th valley is given by $|\alpha^{(j)}|^2$. The hyperfine interaction originates from the localization of the donor electron in the singlet A_1 state. The A_1 state is a product of the ground state $1s$ splitting in the cubic crystal field. The hyperfine splitting is given by the expression $A \sim |\Psi(0)|^2 = |F^{(j)}(0)|^2 |u^{(j)}(0)|^2 |\sum_{j=1}^6 \alpha^{(j)}|^2$. The experimentally observed lowering of A originates from an anisotropic perturbation of the CB bottom. This is due to the asymmetric shape of the nanocrystals; we assume that grains are longitudinal blocks with dimensions $d_\perp \times d_\perp \times d_\parallel$, where the ratio between short and long side is expressed by the parameter $\gamma = d_\perp/d_\parallel$. Throughout the text the sample dimensions are specified by the value d_\parallel . The limited volume and asymmetry of the grain shape produce a tetragonal perturbation of the CB bottom. Due to the restricted volume, the CB minima in perpendicular directions are shifted up more than the CB minima in longitudinal directions. There is a number of publications which derive expressions for enlargement of the energy band gap^{11,23} with diminishing grain size. The en-

largement consists of a downshift of the VB and an upshift of the CB.² Our EPR experiments provide results on the EMT shallow donor, where only perturbation of the CB bottom is significant for the electronic structure of phosphorus. We apply the general formula for the CB upshift²³

$$\Delta E_{\text{CB}} = a/d^b. \quad (1)$$

In our approximation it is assumed that all the grains are oriented in such a way that their longitudinal axis coincides with one of the $\langle 100 \rangle$ crystallographic directions, in analogy to the columnar structure of porous silicon analyzed by theoretical studies. The correlation between the tetragonal perturbation in the valley-orbit matrix and the perturbation induced by spatial confinement takes the form

$$3x\Delta_c \equiv \Delta E_{\text{CB}}(d_\perp) - \Delta E_{\text{CB}}(d_\parallel) = \frac{(1-\gamma^b)a}{\gamma^b d_\parallel^b}, \quad (2)$$

and the value of the parameter is $\Delta_c = 2.17$ meV.²² If we consider that the CB degeneracy lifting affects only the electron probability in the valleys, then the reduction of the hyperfine interaction can be expressed in terms of the $\alpha^{(j)}$, which are functions of the perturbation parameter x . For a more elaborate discussion, see Refs. 20 and 22. The reduction of hyperfine splitting versus perturbation parameter x is given by the expression

$$\frac{A(x)}{A(0)} = \frac{1}{2} \left[1 + \frac{1-x/6}{\sqrt{1-x/3+x^2/4}} \right]. \quad (3)$$

For the largest experimentally found reduction of 6.2%, the perturbation parameter becomes $x = 0.98$. An alternative solution, $x = -1.45$, is not considered here as it corresponds to conduction band downshift.

Since the formulas (2) and (3) combine the hyperfine splitting parameter $A(x)$ and the largest grain dimension d_\parallel with parameters a and b , a fit to experimental data can be performed as is shown in Fig. 4(b). The power dependence of the CB upshift, i.e., the value of parameter b , is found not to be dependent on the particular choice of the asymmetry parameter γ . For the value $\gamma = 0.6$, which has been estimated from the SEM images, we can fit experimental data from the two smallest powders and obtain the parameters describing upshift of CB. It takes the empirical form $\Delta E_{\text{CB}} = 1600/d^{1.1}$, where the ΔE_{CB} is expressed in meV and d in nm. We note that in our approximation we have assumed that the parameter γ did not change upon oxidation.

For large perturbation $x \gg 1$ the EMT predicts reduction of hyperfine splitting to $\frac{1}{3}A(0)$.²² In this range any further upshift of the CB, and thus an increased nonequivalence of the six CB minima, will not affect the hyperfine splitting parameter $A(x)$. In order to estimate the CB upshift in grains of sizes in the range of a few nanometers other experimental techniques would be more appropriate.¹¹

B. Photoluminescence

PL spectroscopy is the most often applied technique in the investigations of spatial confinement effects.^{5,11} For Si

nanocrystals in the few-nanometers range observations of broad bands in the visible region are frequently reported. A pure quantum confinement model predicts that for small enough crystallites radiative recombinations due to the excitonic transitions should appear in the visible region. These should exhibit blue shift upon size reduction. Also the lifetime should decrease with increasing energy of recombination. In the quantum confinement model these effects follow from the fact that the band gap becomes larger and direct. Many of the experimentally observed features have been interpreted along these lines.

There are two major problems in the PL studies conducted on few-nanometer crystallites. The surface-to-volume ratio is so large that surface-related effects dominate PL emission. Secondly, the grain size distribution should be as close as possible to a δ function. In case of grain sizes in the range of a few nanometers band structure perturbation is especially strong. Therefore even a relatively narrow width of size distribution will result in a large spread of exciton energies. For larger crystallites, where the magnitude of band perturbation is smaller, the few-nanometer narrow size distribution is not necessary.

In our research we monitor radiative recombinations which are characteristic for bulk material: a transition from a deep to a shallow state, labeled *D1*, and an electron-hole recombination whose phonon-replicated structure also confirms its bulk origin. Recombination energies of these transitions are traced versus average grain size. On the basis of an observed correlation conclusions concerning size-related effects are drawn.

The PL experiments have been performed in immersed helium, helium-flow and close-cycle cryostats altogether covering the temperature range between $T=4.2$ K and $T=150$ K. For excitation an argon laser operating at $\lambda=514.5$ nm was used. The laser light was mechanically on-off modulated with a frequency of 25 Hz. To record the spectra a germanium detector was used whose operation sensitivity is in the infrared region.

1. Deep-level-related band

A strong, rather broad PL band around 810 meV at $T=4.2$ K, labeled *D1*, has been observed together with other bands *D3* and *D4* at their characteristic positions¹⁴—see Fig. 5(a). They have been reported in the literature and were associated with carrier trapping at dislocations.^{14,24} The bands were not observed in bulk crystal before mechanical deformation. The observation of the *D1* band in the present study is a natural consequence of mechanical breaking used in the preparation of the silicon grains in the ball-milling process. Its broad line width indicates a high density of deformation-induced defects. As measured at $T=4.2$ K the line width of the band is approximately 25 meV. Measurements at higher temperatures have revealed that the *D1* band observed in the studied powders consists of two components at around 775 and 825 meV, respectively [Fig. 5(b)], as observed before by Sauer *et al.*,¹⁴ and Gwinner and Labusch.²⁵ The linewidth of the high-energy line is approximately 30 meV at $T=100$ K. According to the model proposed by Suezawa *et al.*¹⁵ following the earlier interpretation by Gwinner and

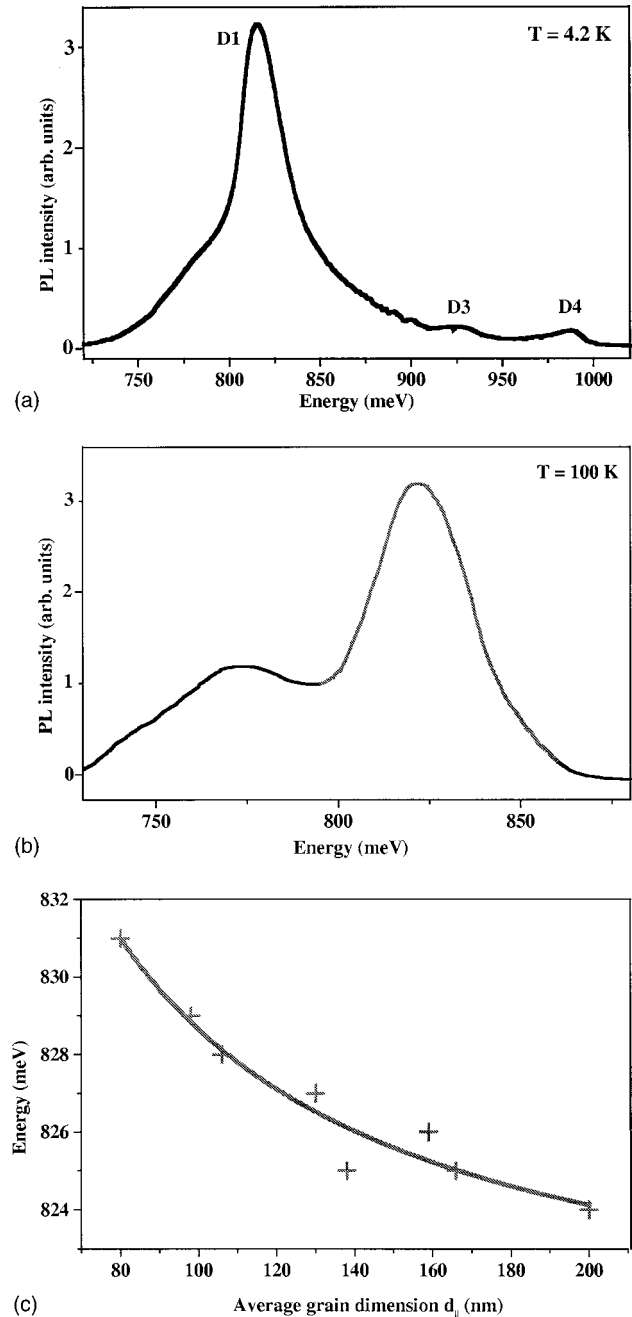


FIG. 5. (a) Photoluminescence spectrum of the *D1* center measured at $T=4.2$ K together with *D3* and *D4* centers. (b) Photoluminescence spectrum of the *D1* center measured at $T=100$ K, consisting of 2 bands: the low-energy component at 775 meV and high-energy component at 825 meV. (c) Energy perturbation of the *D1* band component. Solid line represents the fit with power dependence parameter $b = 1.1$: $E = 1344/d^{1.1} + 820.2$ with E in meV and d in nm.

Labusch²⁵ the transition responsible for the *D1* PL band occurs from a deep level to a shallow acceptor level. Deep levels have usually atomiclike character and therefore show a weaker relation to the band structure of the host than the shallow ones. Deep levels are introduced for example by transition metals and they may serve as a reference in band alignment in semiconductor heterojunctions as demonstrated

by Langer *et al.*^{26,27} Following the model of Suezawa *et al.*¹⁵ the change of transition energy of $D1$, which we observe in experiment can be ascribed mainly to the downshift of the shallow level following the valence band perturbation. Its accurate position has been found by fitting with Gaussian-shape lines. Results show that a correlation exists between the average grain size of the powder and the recombination energy of the high-energy component of the $D1$ band, as plotted in Fig. 5(c). A consistent energy upshift of this transition is found for powders of different initial grain size distributions reduced by oxidation. For the results as presented in Fig. 5(c) the experimental points of the dislocation-related band position have been fitted with the formula for the downshift of VB with the relation $1/d^{1.1}$. The power dependence parameter $b = 1.1$ has been taken equal to that obtained for the CB perturbation for consistency. The fit takes a form $E(\text{meV}) = 1344/d^{1.1} + 820.2$, where d is expressed in nm. Taking into account that the perturbation of energy difference between acceptor level and VB maximum is negligibly small, we find that the VB edge shift is given by $\Delta E(\text{meV}) = -1344/d^{1.1}$. A similar good fit can be obtained setting the power parameter to $b = 2$ which is in agreement with EMT as expected for large grains. This result is an illustration that the experimental data from the PL experiment are not in compelling contradiction with EMT expectations.

2. Dislocation-related PL band

In silicon powders preannealed in an ambient atmosphere prior to oxidation, a strong photoluminescence spectrum as shown in Fig. 6(a) could be observed. A corresponding recombination has not been detected in bulk silicon. Guided by the characteristic properties of the band, such as the energy of the transitions and replicated structure with phonon values of bulk Si we conclude on the electron-hole recombination, where the carriers are trapped at the dislocations. We consider the possibility that the spectrum is due to the impurity-band formation to be less likely. Dedicated SIMS measurements prove that for short oxidation times the pile-up effect of phosphorus donors is negligible (Fig. 3 and Table 1).

The PL emission occurs around $E_{hv} = 1075$ meV in grains of diameter 115 nm. Since the electron-hole binding energy is low $E_{e-h} = 14.3$ meV in comparison to the energy difference between silicon band gap, $E_g = 1170$ meV and emission energy (E_{hv}) we exclude purely excitonic model. To classify the observed luminescence we apply the scheme of Lelikov *et al.* for dislocation-related optical emission.^{28,29} In the general model the radiative transition follows from recombination of a hole and an electron bound in the vicinity of a dislocation. In view of the mechanical treatment of the ball-milled silicon nanocrystals dislocations are widely present to provide such a carrier trapping sites. A diagram of the binding mechanism is illustrated in the work of Lelikov *et al.*²⁸ On the basis of the model the electron-hole recombination energy is derived to be

$$E_{hv} = E_g - A(b_e/a)^2. \quad (4)$$

The emission energy is primarily linked to the bandgap E_g of silicon. Carrier binding reduces the transition energy by

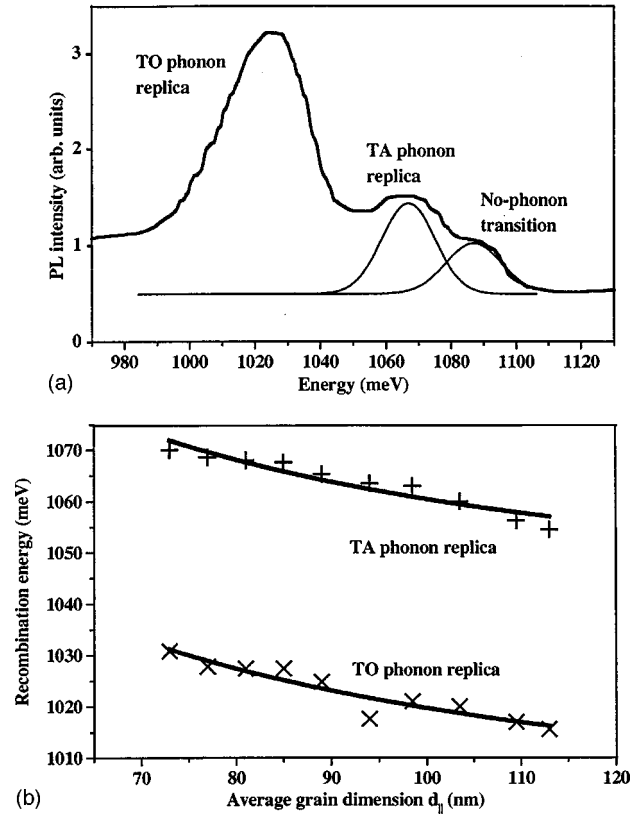


FIG. 6. (a) Electron-hole recombination band investigated in the current study: the no-phonon line followed by TA and TO phonon replicas can be distinguished. (Grain size 80 nm, temperature of measurement is $T = 10$ K.) (b) Parallel energy upshift of TA and TO phonon replicas with diminishing average grain size. Solid lines represent fits with power dependence parameter $b = 1.1$: $E = 4380/d^{1.1} + E_{ph}$ with E in meV and d in nm.

$A(b_e/a)^2$ where b_e is the edge component of the Burgers vector for the given dislocation type and a the crystal lattice constant. Parameter A , depending on carrier masses and deformation potential, has a constant value $A = 800$ meV for silicon. Typical binding energies for the electrons and holes in the dislocation potentials vary from 30 to 400 meV.²⁸ In the present case of nanocrystals the radiative emission occurs approximately 100 meV below the silicon bandgap.

For the investigated band the typical excitonlike emission structure in silicon (indirect band gap material) is observed: no-phonon transition followed by the transverse acoustic (TA) and transverse optical (TO) phonon replicas. These are broad and overlap each other. Their line width is approximately 30 meV, mainly due to the variation of the energy band gap related to the size distribution of grains. The intensity of the TO replica is the strongest in agreement with measurements in bulk silicon. However, the relative intensity ratio NP:TA:TO $\approx 0.25:0.4:1$ is significantly different than for excitonic emission in bulk silicon [Fig. 6(a)]. The separation energy between no-phonon line and phonon replicas matches phonon energies measured in bulk silicon $E_{TA} = 18.5$ meV and $E_{TO} = 58$ meV.³⁰ The presence of phonon replicas shows that the band structure in grains of the order of 100 nm has still indirect character. That is consistent with

theoretical predictions concerning band structure perturbation: upon grain size decrease first the enlargement of band gap magnitude occurs, which is followed by indirect-to direct-gap transition only when the size region of a few nanometers is reached. For the powder of the smallest crystallites with the narrowest grain size distribution, the radiative transition has been observed to shift up in energy with gradually diminishing average grain size, as shown in Fig. 6(b). The observed upshift of TA and TO phonon replicas was parallel in the investigated region. Similar as in the previous case of deep-level-related recombination experimental points for TO and TA phonon replicas have been fitted with a $1/d^{1.1}$ size dependence. As the result of this fit we obtained the following parameters for the change of perturbation $4380/d^{1.1} + E_{\text{ph}}$, where the E_{ph} is the position of TA or TO phonon replica in bulk, d is dimension of the grain expressed in nm, and the energy given in meV. The change observed in the experiment as derived from the fitting formula $4380/d^{1.1}$ was around 14 meV for average grain dimension changing from 75 to 115 nm. A good fit has also been obtained for the EMT formula with power dependence parameter $b=2$. It is an indication that in this range of grain sizes the EMT can also properly describe band structure perturbations. Consequently, in view of the correlation between recombination energy and average grain size, we associate observed upshift with enlargement of the band gap energy due to spatial confinement.

C. Comparison of band shifts

We can compare the independently experimentally determined perturbations of conduction band, valence band and band gap within the investigated range of grain sizes. In case of conduction band the fit has been extrapolated to smaller grains. For grain sizes changing from 120 to 80 nm the increase of conduction band energy, as derived from our empirical formula, is $\Delta E_{\text{CB}} = +4.6$ meV. The change of valence band energy in the same range of grain sizes, as established from the $D1$ band shift, equals $\Delta E_{\text{VB}} =$

-3.9 meV. We note here that according to theoretical calculations of Voos *et al.*,³¹ the downshift of the valence band and upshift of the conduction band are of comparable magnitude. The current experiment gives a similar change for both bands. Taken together the two contributions will give the change of the energy gap of crystallites. On the other hand, from the measurement of the electron-hole recombination we conclude that in the same grain size region the energy gap changes by 12.7 meV. We note that the series of experiments were conducted on individually prepared powder samples that differed in grain size distributions. Taking into account the accuracy of the average grain size estimation, the internal consistency of the experimentally determined band structure perturbations appears to be satisfactory.

IV. CONCLUSIONS

Experimental results, obtained for differently prepared silicon nanocrystalline materials, give evidence of small shifts of the silicon bands induced by spatial confinement. Such effects are shown to appear already for relatively large grains with dimensions of the order of 100 nm. The evidence was obtained by investigating features well known from bulk crystal. Measurements were restricted to relatively large grains for which the spatial confinement effects represent bulk properties and not those of surfaces. Small changes of the conduction band were traced in electron paramagnetic resonance by the reduction of the hyperfine interaction of phosphorus impurity. On that basis an empirical formula for the conduction band upshift is established. A small downshift of the valence band was revealed by the photoluminescence in the dislocation-related $D1$ band. The band gap value of Si grain was independently evaluated by following the recombination energy of an electron-hole transition versus grain size. The experimental results show good qualitative internal consistency. We conclude that the EPR and PL techniques are appropriate tools for investigations of spatial confinement effects in relatively large grains.

¹S. Ögüt, J.R. Chelikowsky, and S.G. Louie, Phys. Rev. Lett. **79**, 1770 (1997).

²N.A. Hill and K.B. Whaley, J. Electron. Mater. **25**, 269 (1996).

³T. Takagahara and K. Takeda, Phys. Rev. B **46**, 15578 (1992).

⁴H. Takagi, H. Ogawa, Y. Yamazaki, A. Ishizaki, and T. Nakagiri, Appl. Phys. Lett. **56**, 2379 (1990).

⁵L.T. Canham, Appl. Phys. Lett. **57**, 1046 (1990).

⁶R. Behrensmeier, F. Namavar, G.B. Amisola, F.A. Otter, and J.M. Galligan, Appl. Phys. Lett. **62**, 2408 (1993).

⁷M.S. Brandt, H.D. Fuchs, M. Stutzmann, J. Weber, and M. Cardona, Solid State Commun. **81**, 307 (1992).

⁸H.D. Fuchs, M. Stutzmann, M.S. Brandt, M. Rosenbauer, J. Weber, A. Breitschwerdt, P. Deák, and M. Cardona, Phys. Rev. B **48**, 8172 (1993).

⁹M. Stutzmann, M.S. Brandt, M. Rosenbauer, H.D. Fuchs, S. Finkbeiner, J. Weber, and P. Deák, J. Lumin. **57**, 321 (1993).

¹⁰T.D. Shen, I. Shmagin, C.C. Koch, R.M. Kolbas, Y. Fahmy, L. Bergman, R.J. Nemanich, M.T. McClure, Z. Sitar, and M.X. Quan, Phys. Rev. B **55**, 7615 (1997).

¹¹Y. Kanemitsu, H. Uto, Y. Masumoto, T. Matsumoto, T. Futagi, and H. Mimura, Phys. Rev. B **48**, 2827 (1993).

¹²Z. Iqbal and S. Vepřek, J. Phys. C **15**, 377 (1982).

¹³N.A. Drozdov, A.A. Patrin, and V.D. Tkachev, JETP Lett. **23**, 597 (1976).

¹⁴R. Sauer, J. Weber, J. Stolz, E.R. Weber, K.-H. Küsters, and H. Alexander, Appl. Phys. A: Solids Surf. **36**, 1 (1985).

¹⁵M. Suezawa, Y. Sasaki, and K. Sumino, Phys. Status Solidi A **79**, 173 (1983).

¹⁶S.-K. Ma and J. T. Lue, Thin Solid Films **304**, 353 (1997).

¹⁷A.S. Grove, O. Leistiko, Jr., and C.T. Sah, J. Appl. Phys. **35**, 2695 (1964).

¹⁸G. Feher, R.C. Fletcher, and E.A. Gere, Phys. Rev. **100**, 1784 (1955).

- ¹⁹W. Kohn and J.M. Luttinger, Phys. Rev. **97**, 883 (1955).
- ²⁰B.J. Pawlak, T. Gregorkiewicz, and C.A.J. Ammerlaan, Physica B **273-274**, 938 (1999).
- ²¹G. Charitat and A. Martinez, J. Appl. Phys. **55**, 909 (1984).
- ²²D.K. Wilson and G. Feher, Phys. Rev. **124**, 1068 (1961).
- ²³V. Ranjan, V.A. Singh, and G.C. John, Phys. Rev. B **58**, 1158 (1998).
- ²⁴R.H. Uebbing, P. Wagner, H. Baumgart, and H.J. Queisser, Appl. Phys. Lett. **37**, 1078 (1980).
- ²⁵D. Gwinner and R. Labusch, Phys. Status Solidi A **65K**, 99 (1981).
- ²⁶J.M. Langer and H. Heinrich, Phys. Rev. Lett. **55**, 1414 (1985).
- ²⁷J.M. Langer, C. Delerue, M. Lannoo, and H. Heinrich, Phys. Rev. B **38**, 7723 (1988).
- ²⁸Yu.S. Lelikov, Yu.T. Rebane, S. Ruvimov, A.A. Sitnikova, D.V. Tarhin, and Yu.G. Shreter, Phys. Status Solidi B **172**, 53 (1992).
- ²⁹Yu. Lelikov, Yu. Rebane, S. Ruvimov, D. Tarhin, A. Sitnikova, and Yu. Shreter, Mater. Sci. Forum **83-87**, 1321 (1992).
- ³⁰G. Davies, Phys. Rep. **176**, 83 (1989).
- ³¹M. Voos, Ph. Uzan, C. Delalande, G. Bastard, and A. Halimaoui, Appl. Phys. Lett. **61**, 1213 (1992).